Colloid Polym Sci (2008) 286:517–524
DOI 10.1007/s00396-007-1795-5

ORIGINAL CONTRIBUTION

Physicochemical characterization of self-assembled poly(∈-caprolactone) grafted dextran nanoparticles

Madhab Prasad Bajgai · Santosh Aryal · Douk Rae Lee · Soo-Jin Park · Hak Yong Kim

Received: 26 June 2007 / Revised: 22 October 2007 / Accepted: 25 October 2007 / Published online: 30 November 2007

Abstract Amphiphilic graft copolymer composed of poly (∈-caprolactone) and dextran was synthesized by ring opening polymerization of ∈-caprolactone initiated through the hydroxyl end of dextran in the presence of stannous 2-ethylhexanoate [Sn $(oct)_2$] as a catalyst. It has been widely characterized by Fourier transform infrared spectroscopy, ^{1}H NMR, and thermogravimetric analysis. Nanoparticles were prepared in aqueous medium by co-solvent evaporation technique at room temperature (25 °C). Hydrodynamic diameter and particle size were measured by dynamic light scattering spectroscopy and atomic force microscopy, respectively. Core-shell geometry of polymeric nanoparticle was characterized by fluorescence spectrophotometer using pyrene as a probe. Critical micelle concentration of polymer in triple distilled water decreased from 6.9×10^{-4} to 8.9×10^{-4} g/l with increasing hydrophobic moiety. Further, the physiological stability of the nanoparticles in phosphate buffer saline of pH 7.4 at 37 °C was evaluated, which showed promising in drug delivery system.

M. P. Bajgai
Department of Bionanosystem Engineering,
Chonbuk National University,
Jeonju 561-756, South Korea

S. Aryal
Center for Healthcare Technology Development,
Chonbuk National University,
Jeonju 561-756, South Korea

D. R. Lee · H. Y. Kim (✉)
Department of Textile Engineering, Chonbuk National University,
Jeonju 561-756, South Korea
e-mail: khy@chonbuk.ac.kr

S.-J. Park
Advanced Materials Division, Inha University,
Jeonju 402-751, South Korea

Keywords Dextran · Graft polymer · Micelles · Nanoparticles · Self-assembled

Introduction

The biodegradable polyesters like poly(ε-caprolactone) (PCL), polylactide (PLA), polyglycolide, and their copolymers have been extensively studied and widely applied in biomedical fields including drug delivery and tissue engineering [1, 2]. Nowadays, polysaccharide-based surfactants derived from block and graft copolymers have attracted much attention not only because of their potential in separation technologies and controlled drug release but also they offer a positive alternative to existing nonbiodegradable formulated system [3]. The most remarkable feature of drug delivery technology is the central role that a polymer plays in the control of drug administration, transport, and delivery at the desired site of action [4]. To address this issue, polysaccharide-based polymers represent an interesting alternative because poly- or oligosaccharides may have, per se, a lot of recognition functions allowing for specific mucoadhesion or receptor recognition. For instance, fucosylated oligosaccharide ligands-mediated cell–cell adhesion through binding to cell surface celectins and galactose containing oligosaccharides have affinity for asialoglycoprotein receptors in liver tumor cells [5, 6]. Among the polysaccharides, dextran has molecular characteristics (hydrophilic and mobility) able to prevent protein opsonization and compliment activation, thus, avoiding liver recognition [3]. Thus, biocompatible polyesters with functionality of polysaccharides should allow the design of ideal material for drug targeting [4].

There are only few studies that mentioned the use of polysaccharides as precursors of macromolecular amphi-

philic architectures; for instance, brush-like poly(L-lactide)-grafted modified dextran have been prepared by initiating ring opening polymerization (ROP) from some free hydroxyl groups of ionic polysaccharides in the presence of stannous octoate [2]. However, engineering the materials for the desire use, here for drug delivery, needs to optimize the conditions that allow amphiphiles to be self-assembled. The fascinating aspect of this system in biomedical field is for increasing drug stability, drug solubility, and transport properties of pharmaceutical materials. The frequently used colloidal nanoparticles are amphiphilic nanoparticles (formed by hydrophobic interaction), polyion complex nanoparticles (resulting from electrostatic interactions), and nanoparticle stemming from metal complexation [5]. Several strategies for the preparation of nanoparticles have been well reported, example includes direct dissolution, solvent evaporation/film formation, dialysis, emulsion, and co-solvent evaporation [7]. Meanwhile, agglomeration is the major problem that needs to control with the use of surfactant or by controlling the fragments of the amphiphile.

Polymers containing at least two distinct blocks (hydrophobic and hydrophilic), covalently bound at one point, lead to form a polymeric nanoparticle via intra- and intermolecular associations between hydrophobic moieties in aqueous medium, as this medium is thermodynamically unfavorable to the hydrophobic segment [8–11]. Polymeric nanoparticles made up of biodegradable block copolymers assembled in their core-shell geometry in which hydrophobic domain (core) serves as a reservoir for the incorporated drugs and hydrophilic domain (shell) as a stabilizing interface of particles, thereby, showing the nature of surfactant [12, 13]. Nevertheless, few studies were devoted to copolymers containing polysaccharides, such as PLA-grafted dextran and PCL-grafted dextran (PGD) via ROP. However, less attention has been given in their aqueous dispersion that results to the formation of polymeric micelles, which could be frequently applied in drug delivery system (DDS). Realizing the importance of aqueous environment for in in vivo application, we herein demonstrated the control synthesis and optimization of the self-assembled polymeric micelles [5].

Experimental

Materials

Dextran was purchased from Pharmacia Biotech, USA, and dried under a reduced pressure at 90 °C for one night and 120 °C for 5 h. ε-Caprolactone (ε-CL; Aldrich, USA) was dried over CaH_2 for 48 h and stored under inert atmosphere. 1,1,1,3,3,3-hexamethyldisilazane (HMDS; 99.9%) was purchased from Aldrich, USA, and used directly. Triethylamine (99%), from Sigma, USA, was dried over barium oxide (BaO) for 72 h, distilled under reduced pressure, and stored under nitrogen atmosphere. Toluene and dimethylsulphoxide (DMSO) were refluxed over CaH_2, tetrahydrofuran (THF) over Na/benzophenone, and all the solvents were stored under nitrogen atmosphere.

Silylation of dextran

Dextran was dissolved in DMSO along with the addition of desired quantity of triethylamine and silylating agent under a nitrogen flow with previously dried syringes. The reaction condition was kept at 60 °C for 48 h. Calculated amount of THF and toluene were added to make the reaction condition homogenous during silylation. After the completion of the reaction, the silylated dextran was precipitated in cold water, dried in a vacuum, and distilled azeotropically three times in toluene. Protection yield was calculated by ^{1}H NMR as described earlier using Eq. 1 [9].

$$\text{Yield}\,\% = \frac{A_{\text{OSiMe3}}}{A_{\text{glycosidic H}}}\ \frac{6 \times 100}{27} \tag{1}$$

Where A_{OSiMe3} and $A_{\text{glycosidicH}}$ are the respective areas of trimethylsilyl group at 0.15 ppm and glycosidic proton centered at 3.2 to 4.2 ppm. The degree of substitution was calculated as Eq. 2:

$$\text{DS} = \frac{3\text{yield}(\%)}{100} \tag{2}$$

Polymer synthesis

In a typical experiment, the remaining hydroxyl group acts as a macro-initiator and subjected for the ROP of ε-CL in the presence of stannous octoate. The polymerization was carried under nitrogen at 150 °C for 48 h. The reaction product was recovered by precipitation in heptane and dried under vacuum. Silylated graft copolymer was dissolved in THF and added to the dilute aqueous solution of 1 M HCl with respect to the number of $-OSiMe_3$ functions at room temperature. The deprotected copolymer was recovered by precipitation in heptane and dried under vacuum. Three different types of PGD (PGD20, PGD30, and PGD-50) with different molecular weight were synthesized (Table 1).

Polymer characterization

^{1}H NMR spectra of the samples were recorded by using JNM–Ex 400 FT–NMR spectrometer (Jeol, Japan), operating at 400 MHz, 6%(^{1}H) (*w*/*v*) sample solution in $CDCl_3$ and d_6-DMSO using tetramethylsilane (TMS) as an internal reference. Fourier-transform infrared (FT-IR) spectra were

Table 1 Characterization of PGD polymers

Sample	Feed ratio (CL/OH)	Mol. wt.	F_{PCL} ^{1}H NMR	Td[1] (°C)	Td[2] (°C)
PGD20	20	14,100	0.94	355	420
PGD30	30	20,300	0.96	427	–
PGD50	50	32,900	0.98	430	–

recorded as KBr pellets using an ABB Bomen MB100 Spectrometer (Bomen, Canada). Gel permeation chromatography measurements were made via a Waters 150C apparatus equipped with a refractive index detector and waters styragel® columns (HR_1, HR_2, and HR_4; Polymer Laboratories, England) with a size of 7.8×300 nm, using chloroform as an mobile phase at the flow rate of 1.0 ml/min. TGA was performed by a Perkin–Elmer TGA 6 thermogravimetric analyzer (Perkin–Elmer, USA) equipment under a nitrogen atmosphere. The experiments were performed at a heating rate of 10 °C/min in the range of 50–600 °C. Differential scanning calorimetric (DSC) analysis of polymer was performed by a DSC Q100V 7.3 build 249(Perkin–Elmer, USA) at a heating rate of 20 °C/min in the range of −60 to 150 °C under the steady flow of nitrogen.

Preparation PGD nanoparticles

PGD nanoparticles were prepared in triple distilled water using co-solvent evaporation technique. The polymer (10 mg) was dissolved in acetonitrile (1.0 ml) and dropped into 10 ml of triple distilled water under moderate stirring (50 rpm) at room temperature. The organic phase was allowed to evaporate under reduced pressure until the final volume of the aqueous suspension was reduced to 10 ml. Finally, the suspension was filtered by a microfilter with a 0.2-μm pore size to remove any polymer aggregates. Furthermore, to measure the physiological stability, the particles were prepared in phosphate-buffered saline (PBS) at pH 7.4 accordingly.

Nanoparticle characterization

Critical micelle concentration (CMC) of the polymeric nanoparticles was measured by steady-state pyrene fluorescence method. Steady-state fluorescent excitation spectra (λ_{em}=390 nm) of pyrene were measured at various polymer concentrations using F-200 fluorescence spectrometer 2510221-07 (Hitachi, Japan). Concentrations of polymer were in the range of 1×10^{-4} to 1 g/l and 6×10^{-7} g/l in triple distilled water at constant pyrene concentration (1×10^{-7} M). CMC value of the polymeric nanoparticle was determined using intensity ratio of band 337 nm to the 334 nm of pyrene in excitation spectra. The intensity ratio of I_{337}/I_{334} against polymer concentration (log c) in pyrene excitation spectra was plotted. Size and surface morphology of the polymeric nanoparticles were observed by AFM nanoscope IV multimode (Digital Instrument, MicroMash, USA) in tapping mode using Si cantilever with a spring constant of 305 N/m and a resonance frequency of 75 kHz. Scanning was performed at scan speed of 1.85 Hz. Samples for AFM observation were prepared as a drop-coated film on the argon dried Si (1,1,1) wafers. Furthermore, morphological examination of the copolymer micelles was performed using a H7650 transmission electron microscope (TEM; BioTem, Hitachi, Japan). A drop of PGD50 copolymer aqueous solution (1 mg/ml) was dropped into a 400-mesh copper grid coated with carbon and was stained with phosphotungstic acid. The sample was dried before TEM observation. Average particle size and size distribution was determined by DLS (Malvern System 4700 instrument) equipped with vertically polarized light supplied by argon ion laser (Cryonics) operated at 20 mW. All experiments were performed at room temperature (25 °C) of measuring angle 90 ° to the incident beam. ζ-Potential of the nanoparticles was determined by elastic light scattering (ELS) measurement (ELS 8000/6000 Otsuka Electronics, Japan) at 25 °C with a measuring angle of 20 ° when compared to the incident beam. Before analysis, samples were sonicated in an ultrasonicator bath for 1 min.

Results and discussion

Silylation of dextran

HMDS is the best choice for controlled silylation of hydroxyl function because of the obtainment for high protection yield and no degradation of dextran chain unlike chlorotrimethylsilane (TMSCl) [9]. Addition of triethyl amine increased the silylated yield. Here, we have obtained the degree of substitution 2.5 by the ^{1}H NMR. Although the protection yield also depends on various other parameters like duration of reaction, reaction temperature, HMDS/OH molar ratio, the reaction at low temperature even at longer period gives poor yield. It is explained as because of the fact that, as silylation proceeds the reaction, the medium became more and more heterogeneous [14]. In the first step, silylation reaction was carried out in DMSO as the solubility preference of dextran. After 4 h of reaction, toluene and THF were added to the reaction mixture to maintain the homogenous condition. The silylation reaction was carried at 60 °C for 48 h. After precipitation in cooled water, the silylated derivative was dried in oven and characterized as 83.6% protection yield and 2.5 degree of substitution as calculated by ^{1}H NMR (Fig. 1).

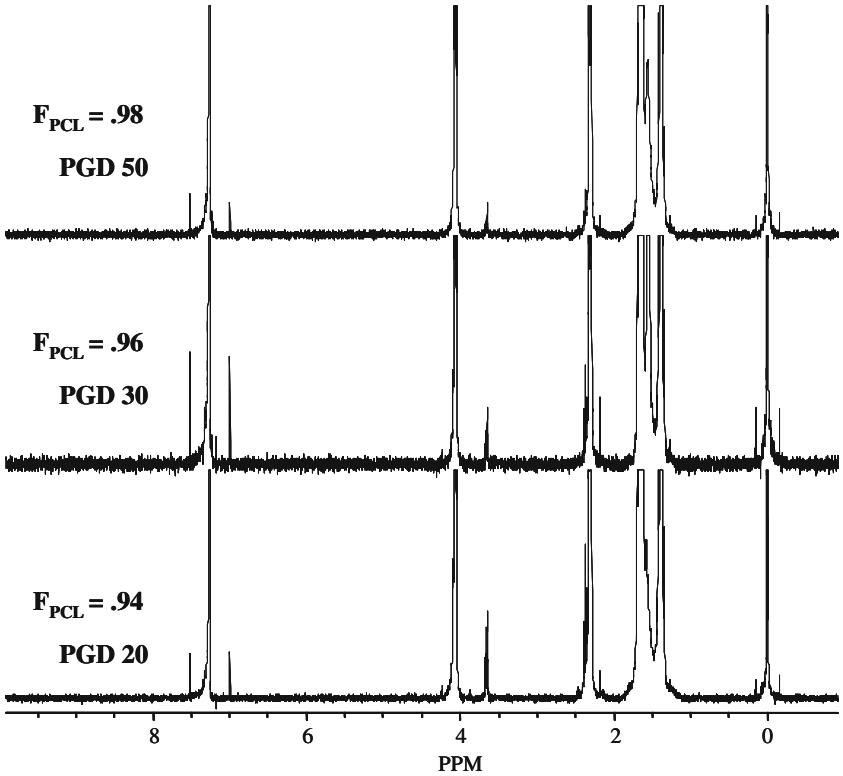

Fig. 1 ^{1}H NMR spectrum of PGD copolymer

Synthesis of polyester-grafted dextran

The remaining free hydroxyl groups, which act as a macro-initiator, are activated by catalytic amount of stannous octoate (Sn (Oct) $_2$) in toluene at 100 °C followed by polymerization with a calculated amount of ∈-caprolactone at 150 °C for 48 h. The resulting grafted copolymer was characterized by higher molecular weights than the starting partially silylated dextran multifunctional macro-initiator. Furthermore, the molecular weight distribution of the grafted copolymer was symmetrical with a polydispersity index around 1.6. The polyester weight fraction F_{PCL} in the copolymer was determined with the help of ^{1}H NMR by comparison of the relative areas of the {–CH_2–O–C(O)–} ester methylene protons at 4.1 ppm and from the {–O–C(O)–CH_2–} α-carbonyl methylene protons at 2.3 ppm and, on the other side, the glycosidic methane and methylene protons in the range 3.2 to 4.2 ppm and the value obtained in the range 0.94–0.98 [3]. This leads to the higher F_{PCL} values than the value obtained gravimetrically, more practically for copolymers rich in PCL. It is assumed that there is some restriction of chain backbone mobility because the numerous polyester grafts might be responsible for the partial screening of the glycosidic protons in ^{1}H NMR spectra measured at higher temperature [3]. Taking into account this observation, one may assume the formation of a quite stable core-shell confirmation [15] and as a result of the introduction of voluminous PCL grafts spread all along the silylated dextran backbone[3]. The final step of polymer synthesis consists of the removal of trimethyl-protecting groups by the treatment of the graft copolymers in the THF solution with a slight excess of an aqueous HCl (1 M). Complete deprotection has been demonstrated by FT-IR spectroscopy, the disappearance of absorption bands of the trimethylsilyl functions at the benefit to a large absorption at approximately 3,500 cm^{-1}, typical of hydroxyl groups (Fig. 2). As expected, the six absorption bands related to trimethylsilyl groups at 750, 842, 874, 1,020, 1,156, and 1,250 cm^{-1} have disappeared.

Thermal analysis

TGA is the best method for characterizing copolymers [16–18]. Polymeric composition can be obtained by degradation process illustrated by the inflection temperature (Td; Fig. 3). TGA thermograms of low PCL content (F_{PCL} 20) showed double degradation phenomena because of pyrolysis of each component, polysaccharide and polyester. Upon increasing the PCL content (F_{PCL} 30 and F_{PCL} 50), the resulting polymer is found to be more homogeneous and exhibit single inflection point temperature (Td; Table 1). Pyrolysis of PGD occurred at lower temperature than that of pure PCL, probably, as a consequence of interactions occurring between PCL and degradation products from the natural component.

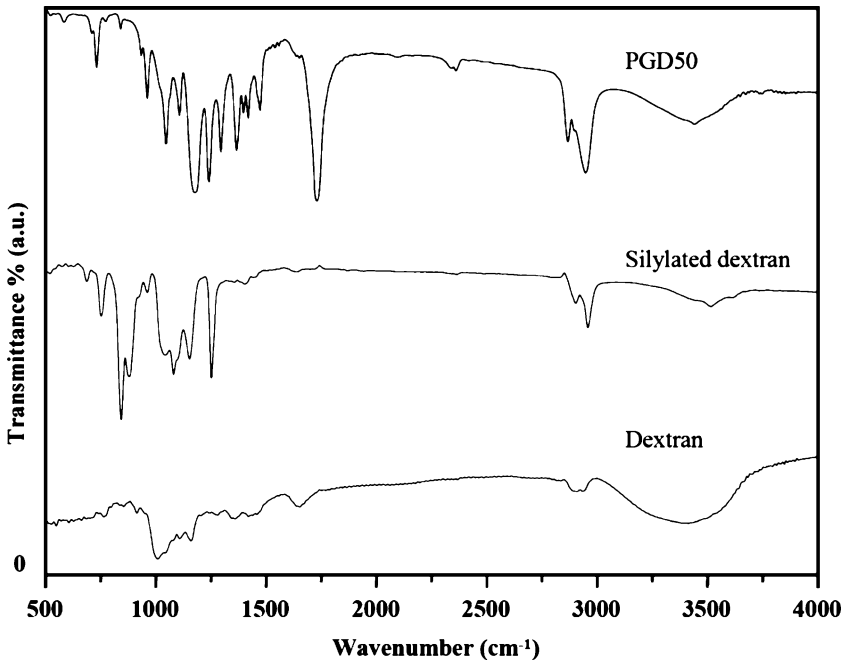

Fig. 2 FT-IR spectra recorded from KBr plate

Determination of CMC

Different methods have been used to prepare polymeric nanoparticles, for example, direct dissolution, solvent evaporation/film formation, dialysis, and co-solvent evaporation [7, 8]. Selection of any methods depends upon factors such as particle size requirement, thermal, and chemical stability of the active agent, reproducibility of the release kinetic profiles, and residual toxicity associated with the final product. In the present study, we have selected co-

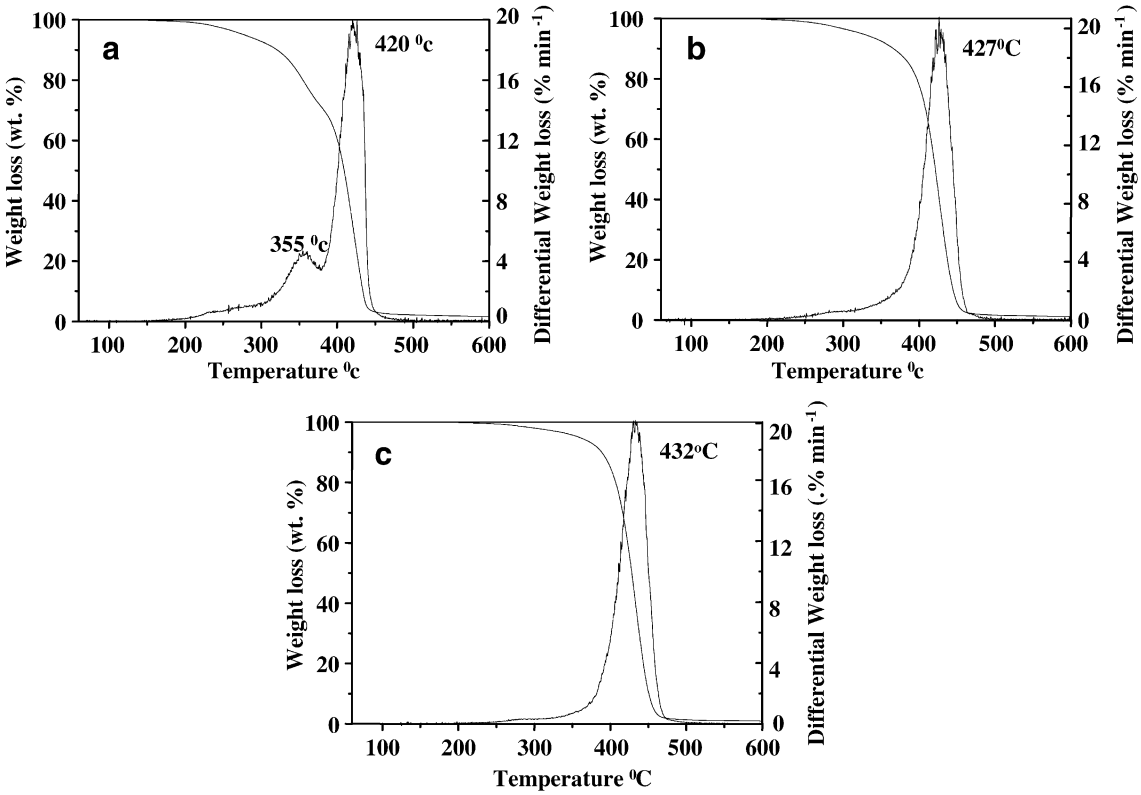

Fig. 3 TG curve obtained by heating the samples from 50 to 600 °C at 15 °C/min under the steady flow of nitrogen **a** PGD 20, **b** PGD 30, and **c** PGD 50

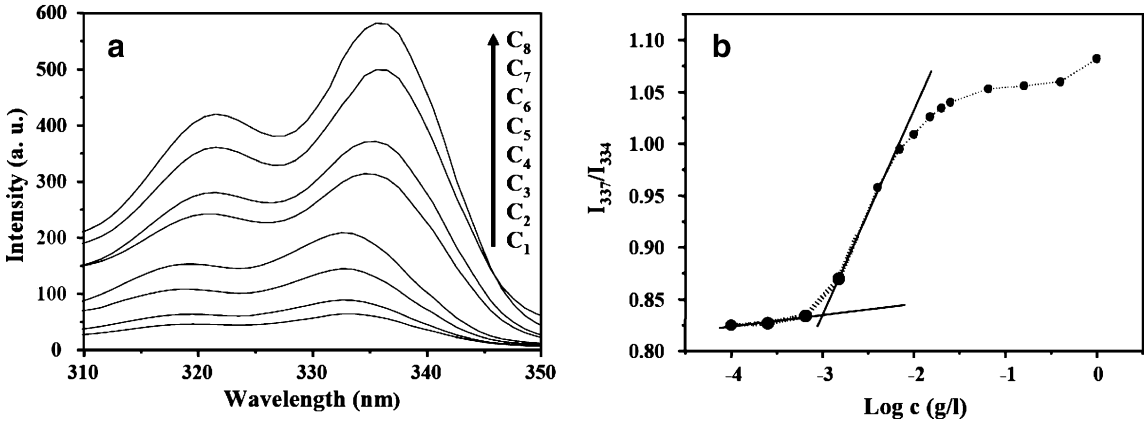

Fig. 4 **a** Fluorescence excitation spectra of pyrene as a function of PGD 50 nanoparticles concentration; 0.0001 (C_1), 0.00065 (C_2), 0.0015 (C_3), 0.004 (C_4), 0.01 (C_5), 0.025 (C_6), 0.160 (C_7), 1.0 (C_8) mg/ml distilled water (λ_{em}=390 nm) and **b** intensity ratio (I_{337}/I_{334}) from pyrene (6×10^{-7} m) excitation spectra (λ_{em}=390 nm) vs nanoparticles concentration (log c) in distilled water

solvent evaporation technique (acetonitrile/water system) for the purpose, as organic solvent of this system can be easily removed at room temperature [7]. Stability of the nanoparticle was increased with the fraction of PCL. No doubt, the semicrystalline nature of PCL that enables the penetration of the water molecules in the system consequently leads the destabilization of nanoparticles; however, hydrophilic brush provides a polymeric net around the core, thereby, preventing it from possible corrosion. The insight location of hydrophobic segment at this stage is well characterized by fluorescence spectra using pyrene as a fluorescence probe [7, 11]. Figure 4 shows the typical fluorescence spectra of pyrene in aqueous medium. The characteristic feature of pyrene excitation spectra was a linear red shift of band from 334 to 337 nm with the concentration of the polymers. The CMC at this stage is summarized in Table 2. The linear red shift was because of the fact that pyrene was preferentially partitioned into hydrophobic domain and moved from the polar environment to the hydrophobic micelle cores as the micelles were formed. The graft copolymer having a higher degree of substitution (DS) formed more rigid or compact hydrophobic core in self-aggregates with polarization. The result indicates that the formation of nanoparticle is facilitated by the hydrophobicity of the polymer. Although there is not much variation in CMC, the cloud stability was more than 2 months as indicated by constant DLS data.

Table 2 Characteristic features of PGD nanoparticles

Sample	Particle size (nm)		ζ-Potential (mV)	CMC (g/l)
	Mean ± SD AFM	DLS[a]	Mean ± SD	Mean ± SD
PGD 20	55±0.3	128±5	−30±0.14	6.9×10^{-4}
PGD 30	48±0.4	110±4	−42±0.35	7.3×10^{-4}
PGD 50	36±0.2	80±2	−50±0.12	8.9×10^{-4}

[a] No variation was found after 2 months of storage at 4 °C.

Morphology and particle size determination

Morphology and size of the polymeric nanoparticles analyzed by AFM and DLS measurement and observation are summarized in Table 2. AFM observations revealed that most of the particles from all the samples were discrete smooth and regular with 30- to 50-nm diameters (Fig. 5). DLS measurement showed a unimodel size distribution with a mean hydrodynamic diameter in the range of 80–128 nm (Table 2). The linear decrease in particle size with the fraction of PCL was in good agreement with the AFM observation. This may be caused by the remarkable solubilization and hydrophobic effect of PCL found to depend on the F_{PCL} (Fig. 6). Subsequently, the study was carried out on the morphology of micelles by the use of TEM. It can be confirmed that the resulting polymeric micelles in water are spherical in shape (Fig. 7), with the diameters ranged from 30 to 60 nm. Furthermore, the stability of the particles was measured by incubating particles at 37 °C in PBS at physiological condition (Fig. 6). This stability study of the particles prepared in PBS reveals that particles hold promise in delivery system. As demonstrated in Fig. 6, one can find that the size of nanoparticles has been altered. This is because of the aggregation of degraded products [19]. Presumably, with incubation time, the degradation of core PCL enhanced and could loosen the aggregation, thereby, destroying the self-assembly. However, this phenomenon might show the low effect with high content of PCL. Also, slow degradation rate of PCL support the evidence [20]. The wide variation in particle size measured by AFM and DLS was because of the fact that DLS measurements give only

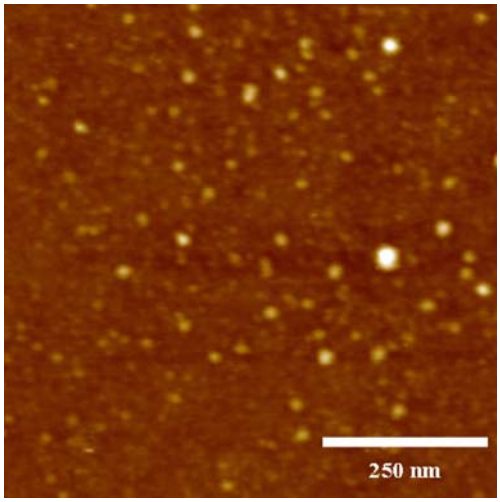

Fig. 5 AFM image recorded from the drop cast film of PGD 50 nanoparticles dispersed in distilled water (1 mg/ml)

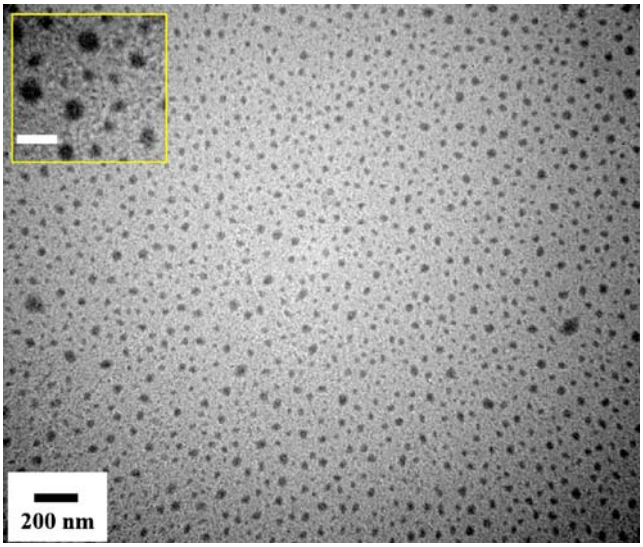

Fig. 7 Transmission electron microscopy micrographs of the PGD50 copolymer micelles. *Inset* is the high magnification image (scale bar is 100 nm)

the hydrodynamic diameter rather than the actual diameter of the nanoparticles. ζ-Potential at this stage was found to be negatively correlated with PCL. However, constancy in ζ-potential (−30 to −50 mV) on varying the PCL content suggests the uniformity in particle size in all polymeric proportions (Table 2) [8]. Although the fraction of ionizable carboxyl group varies in different formulations, the homogeneity in the core controls the constancy of the particle potential. It implies that the micelle yield drug loading content and entrapment efficiency of PGD polymeric nanoparticle could be significantly enough.

Conclusion

In the present study, amphiphilic graft copolymers composed of poly(∈-caprolactone) and dextran have been successfully synthesized. The physicochemical characterizations of self-assembled polymeric nanoparticles have been studied. TGA exhibited that PGD was modified into a semicrystalline and high flexible state with the presence of PCL fraction. DLS measurement showed that the particle size was less than 128 nm, and the hydrophobic segment

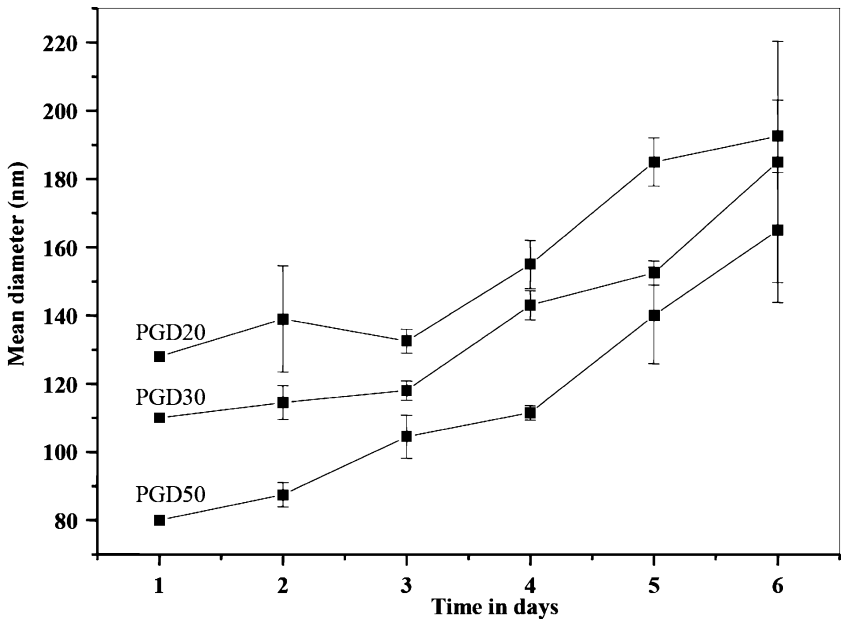

Fig. 6 Stability of the particles measured by measuring change in particle size with incubation time. Particles were incubated at 37 °C in PBS at physiological condition

makes a significant influence on the mean diameter. CMC was linearly decreased with increasing the $F_{PCL,}$ thereby, decreasing particle size. Nanoparticles contained an established composition of PCL as the solid core, along with dextran as a stabilizer corona. The strong hydrophobic interaction of PCL would facilitate the aggregate formation and reduces CMC with respect to F_{PCL}. The investigation for the polymeric nanoparticles into an aqueous medium showed that the composition of the hydrophobic segment makes a significant influence on its physicochemical characteristics. Thus, formulated nanoparticles could give reasonable drug release profile and would hold the promise in drug delivery system.

Acknowledgment This research was supported by the Korean Research Foundation (KRF2007-211-D00032), grant funded by the Korean Government (MOEHRD), Korean Government project no. 10028211 through the Ministry of Commerce, Industry and Energy Department and Regional Research Centers Program of the Korean Ministry of Educational and Human Resources Development through the Center for Healthcare Technology Development, Chonbuk National University, Jeonju 562-756, Republic of Korea.

References

1. Riva R, Schmeits S, Christine J, Robert J, Philippe L (2007) Macromolecule*s* 40:796
2. Nouvel C, Dubois P, Dellacherie E, Six JL (2004) J Polym Sci A Polym Chem 42:2577
3. Ydens I, Rutot D, Philippe D, Six JL, Dellacherie E, Dubois P (2000) Macromolecules 33:6713
4. Gref R, Rodrigues J, Couvreur P (2002) Macromolecules 35:9861
5. Listinski JJ, Siegal GP, Listinski C (1998) Am J Clin Pathol 110425:440
6. Stahn R, Zeisig R (2000) Tumor Biol 21:176
7. Remant KC, Bhattarai SR, Aryal S, Khil MS, Dharmaraj N, Kim HY (2007) Colloid Surf A Physicochem Eng Aspects 292:69
8. Semenov AN, Joanny JF, Khokhlov AR (1995) Macromolecules 28:1066
9. Kazunori K, Harada A, Nagasaki Y (2001) Adv Drug Deliv Rev 47:113
10. Allen C, Maysinger D, Eisenber A (1999) Colloid Surf B Biointerfaces 16:3
11. Nakanishi T, Fukushima S, Okamoto K, Suzuki M, Matsumura Y, Yokoyama M, Okano T (2001) J Control Release 74:295
12. Caroline L, Couvreur P, Besnard M, Cstantini D, Gref R (2003) Pharm Res 20:1284
13. Karin DF, Wensink V, Jiang X, Schotman G, Kruijtzer G, Redenberg A, Chung JT, Zhang Z, Versluis C (2006) Biomacromolecules 7:2983
14. Nouvel C, Dubois P, Dllacherie E, Six JL (2003) Biomacromolecules 4:443
15. Kim K, Kwon S, Park JH, Chung S, Jeong SY, Kwon IC (2005) Biomacromolecules 6:1154
16. Bhattarai N, Kim HY, Lee DR, Park SJ (2003) Polym Int 52:6
17. Bhattarai N, Bhattarai SR, Khil MS, Lee DR, Kim HY (2003) Eur Polym J 39:1603
18. Bhattarai N, Kim HY, Lee DR (2002) Polym Degrad Stab l78:423
19. Chunhua S, Shengrong G, Chengfei Lu (2007) Polym Degrad Stab 92:1891
20. Hongfan S, Lin M, Cunxian S, Xiumin C, Pengyan W (2006) Biomaterials 27:1735